The Pharmaceutical and Chemical Journal, 2016, 3(4):48-57

Available online www.tpcj.org

Research Article

ISSN: 2349-7092
CODEN(USA): PCJHBA

Binding thermodynamic and spectroscopic of Allura Red AC to Calf thymus DNA

Sahar Alamatsaz, Nahid Rasouli*, Nasrin Sohrabi

Department of Chemistry, Payame Noor University, PO Box 19395-3697, Tehran, Iran

Abstract The binding behaviour of an azo dye, Allura Red AC with calf thymus deoxyribonucleic acid (ct-DNA) was investigated using UV-vis absorption spectroscopy, fluorescence quenching method, DNA melting and viscosity measurement. The physicochemical characteristics of Allura Red AC were investigated in 5 mM aqueous phosphate buffer of pH 7.0 at 25 ℃. Spectrophotometric studies of the interaction between Allura Red A C and ct-DNA have shown that the binding constant was K_b=7.5×10^5 M^{-1} at 298 K. Thermodynamic parameters indicated that hydrogen bond and van der Waals play major roles in the interaction. A competitive binding with ethidium bromide (EB) showed that Allura Red AC displace EB from its binding site in ct-DNA. The thermal denaturation experiments show the melting temperature of ct-DNA increases (about 5.0 °C) due to binding of Allura Red AC. There is no obvious increasing of ct-DNA viscosity was observed. All of the experimental results show that the groove binding must be predominant.

Keywords Azo dye; Calf thymus DNA; binding; Thermodynamic; fluorescence quenching.

Introduction

Deoxyribonucleic Acid (DNA plays major roles in many biological processes such as gene expression, transcription, mutagenesis and carcinogenesis [1-2]. Therefore, study on the interaction of small molecules with DNA has been an important research field [3-8]. Generally, the small molecules can bind to DNA by non-covalent interactions such as the π-stacking, hydrogen-bonding, van der Waals, the electrostatic and hydrophobic forces [9-10]. The azo dyes as the main important class of synthetic dyes account for more than 50 % of all the dyes and more than 2000 different azo dyes used annually in various fields [11-15].

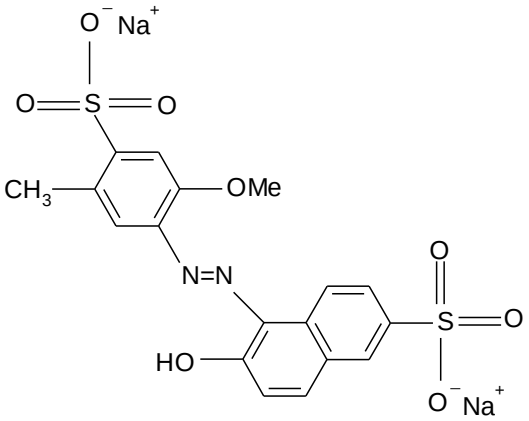

Figure 1: The molecular structure of Allura Red AC

The azo dyes containing azo (-N=N-) functional groups and aromatic ring are reductively cleaved into aromatic amines such as benzidine with toxic, mutagenic and carcinogenic properties [16-19]. So, studies on the binding mechanism between azo dyes and biological molecules are of great importance in the fields of environment and molecular biology. Allura Red AC (Figure 1) is a synthetic azo dye that used as color additive in foodstuffs and cosmetics [20, 21]. Recently, the toxic effects of several food colorants have been investigated and shown to be toxic [22]. To the best of our knowledge; the binding of Allura Red AC with deoxyribonucleic Acid (DNA) has not been reported. So, in the present work, we have investigated the interactions of Allura Red AC with ct-DNA using Spectrophotometric, fluorimetric, viscosity and thermal denaturation measurement. These studies provide an understanding of the binding affinity of Allura Red AC to ct-DNA.

Experimental Work

Materials and Instruments

Calf thymus DNA and Allura Red AC were purchased from Sigma Chemical Company and was used without further purification. All experiments were performed in 5 Mm phosphate buffer solution at pH 7.0 at 25 °C. The concentrations expressed in moles of base pairs per liter were obtained using $\varepsilon = 1.32 \times 10^4$ $L.mol^{-1}.cm^{-1}$ at the absorption maximum of 260 nm. The electronic absorption spectra were measured by a UV-vis Perkin Elmer Lambda 25 double beam spectrophotometer. The fluorescence spectra were determined by a Hitachi MPF-4 spectrofluorimeter. The Melting experiments were performed using an UV-vis Perkin Elmer Lambda 25 double beam spectrophotometer coupled with a thermostated cell compartment. The temperature inside the cuvette was determined with a platinum probe and was increased over the range 25-86 °C by a heating rate of 0.5 °C/min (Thermal software). The viscosity of ct-DNA solutions was measured using an Ostwald viscometer at 25 ± 0.1 ^oC. In all of the experiments, we used a potentiometer Metrohm744-model for measuring pH.

Results and Discussion

UV-vis absorption spectroscopy

At first, the physicochemical characteristics of Allura Red AC were investigated at various concentrations of Allura Red AC and ionic strength (NaCl) in 5 mM aqueous phosphate buffer of pH 7.0 at 25℃. The absorption spectrum of the Allura Red AC dye exhibits a strong absorption band in the visible region at λ_{max} = 504 nm that is related to the azo (-N=N-) functional group [23]. In the presence of increasing amounts of Allura Red AC, no change in the shape of absorption band and the maximum of wavelength can not been observed (Fig.2).

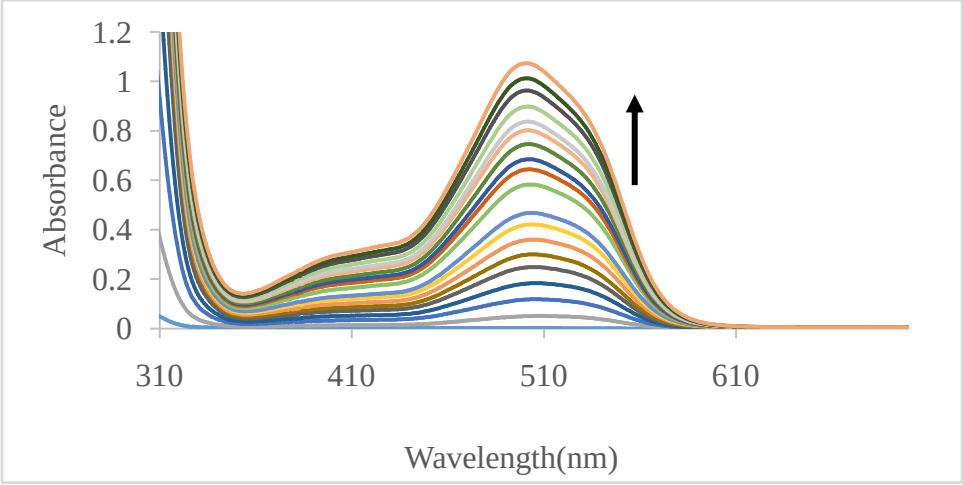

Figure 2: Absorption spectra of Allura Red AC solution (2×10^{-5} M) in the presence of increasing amount of Allura Red AC concentrations [2.95×10^{-7} M, 7.6×10^{-7} M, 2.4×10^{-6} M, 7.6×10^{-6} M, 1.38×10^{-5} M and 2.26×10^{-5} M]. Arrow shows the absorbance changes upon increasing dye concentrations.

Also, the results showed that the absorption in the λ_{max} = 504 nm of Allura Red AC and in the concentration range of 0 to 4.47×10^{-5} M obeys from Beer's law (Fig.3).

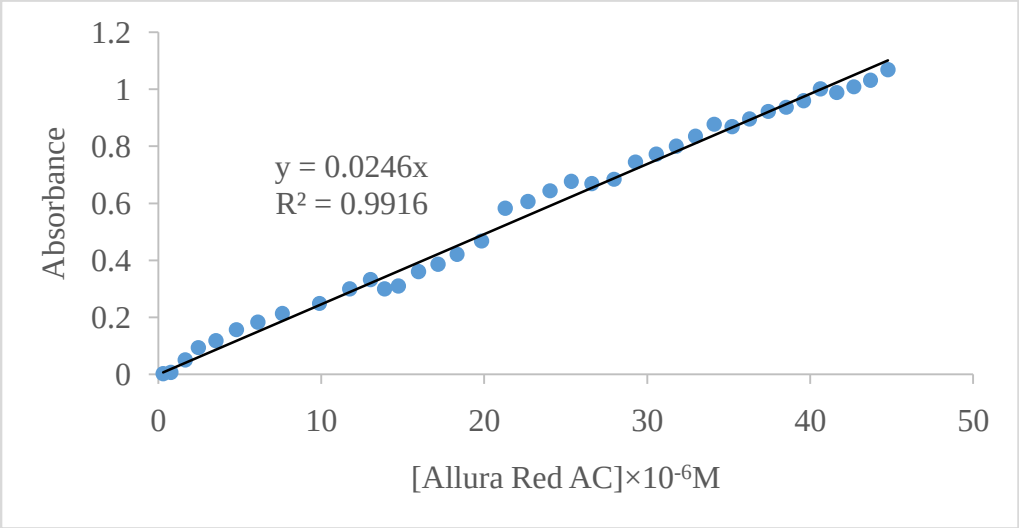

Figure 3: The absorption in the λ_{max}= 504 nm of Allura Red AC obeys from Beer's law in the concentration range of 0 -4.47×10^{-5} M.

Also, the effect of NaCl salt on the absorption spectrum of aqueous solution of Allura Red AC is shown in Fig. 4. The absorbance at all of the spectral regions of studied azo dye has been decreased due to increasing of NaCl concentration and this hypochromocity for Allura Red AC spectrum is accompanying with blue shift. From these results it can be concluded that Allura Red AC forms defined aggregate (H or J aggregate) at high concentration of salt [24-26].

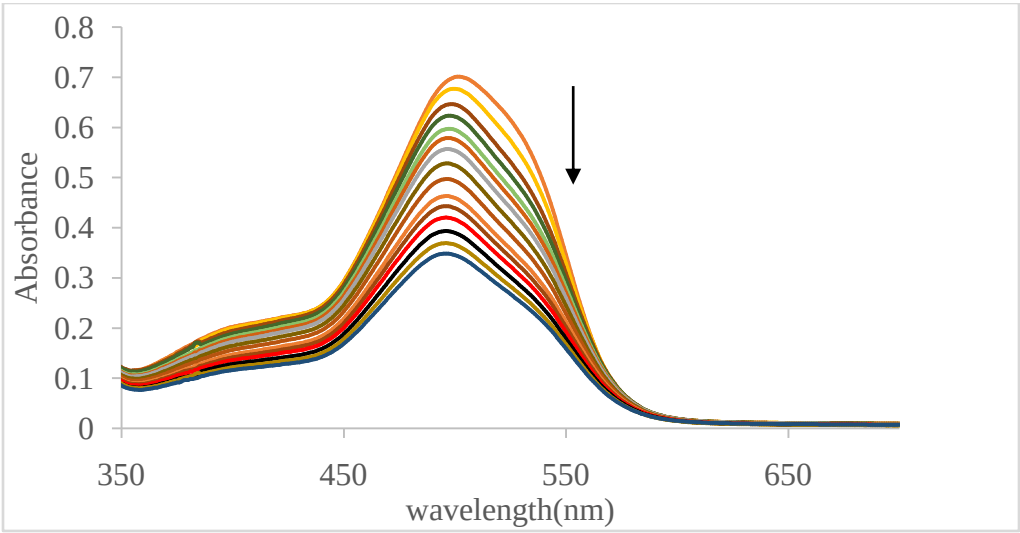

Figure 4: Absorption spectra of Allura Red AC solution (2 × 10^{-5} M) upon addition of NaCl in 5 mM phosphate buffer, pH 7.0 at 25 °C. Arrows indicate the change in absorbance upon increasing the NaCl concentration

In order to investigate the binding behavior of Allura Red AC and ct-DNA, the absorption titration experiments are performed with fixed concentrations of the Allura Red AC (4.5×10^{-5} M), while gradually increasing the concentration of ct-DNA (0-1.3×10^{-4} M) at 25 °C. The absorption spectra of the Allura Red AC in the presence of various ct-DNA concentrations are shown in Fig. 5.

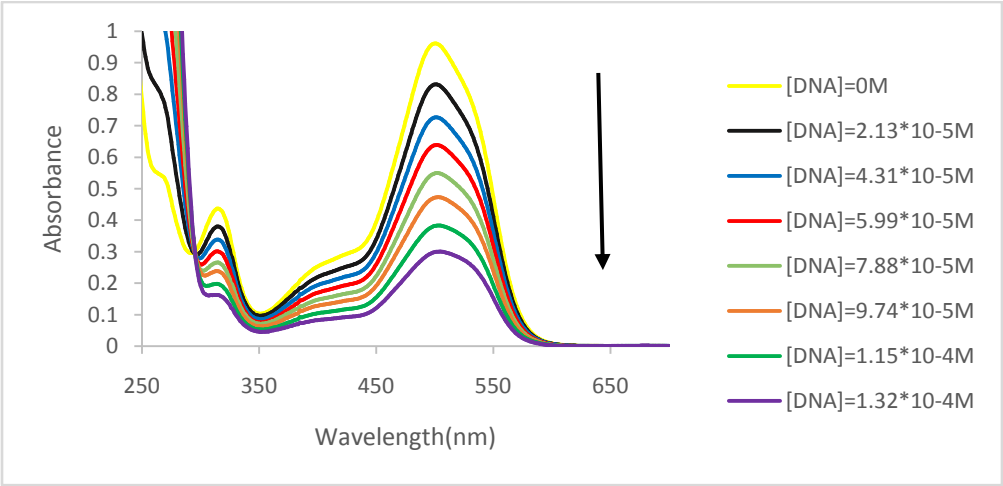

Figure 5: Absorption spectra of Allura Red AC solution (4.5 × 10^{-5} M) upon titration with stock solution of ct-DNA in 5 Mm phosphate buffer, pH 7 and at 25 °C, DNA concentrations are: 0; 7.6 × 10^{-6} M; 2.7×10^{-5} M; 7.6×10^{-5} M; 8.6×10^{-5} M; 9.7×10^{-5} M and 1.3×10^{-4} M. Arrows indicate the changes in absorbance upon increasing the ct- DNA concentration.

As can be seen, upon addition of increasing amount of ct-DNA, a significant "hypochromic" effect was observed in all spectral region. Also, the existence of an isosbestic point in the 295 nm wavelength indicates the formation of ground state complex between Allura Red AC and ct-DNA. The intrinsic binding constants (K_b) of the Allura Red ACwith ct-DNA were determined using Eq. (1) [27-31]:

$$[\text{ct-DNA}]/(\varepsilon_a-\varepsilon_f) = [\text{ct-DNA}](\varepsilon_b-\varepsilon_f) + 1/K_b\,(\varepsilon_b-\varepsilon_f) \quad (1)$$

Where ε_a, ε_f and ε_b corresponded to the apparent extinction coefficient, the extinction coefficient for the free and bound complex absorptivity, respectively. In the plots of [ct-DNA]/(ε_a-ε_f) versus [ct-DNA], K_b was given by the ratio of the slope to intercept (Fig. 6). The binding constant was calculated to be 7.5×10^5 M^{-1}. Moreover, the K_b value obtained was lower than that of classical intercalators [32], whose binding constants are on the order of 10^6-10^7. Comparing the intrinsic binding constant of the Allura Red AC with those of known DNA groove binders we can deduce that this complex binds to ct-DNA *via* groove binding mode [33].

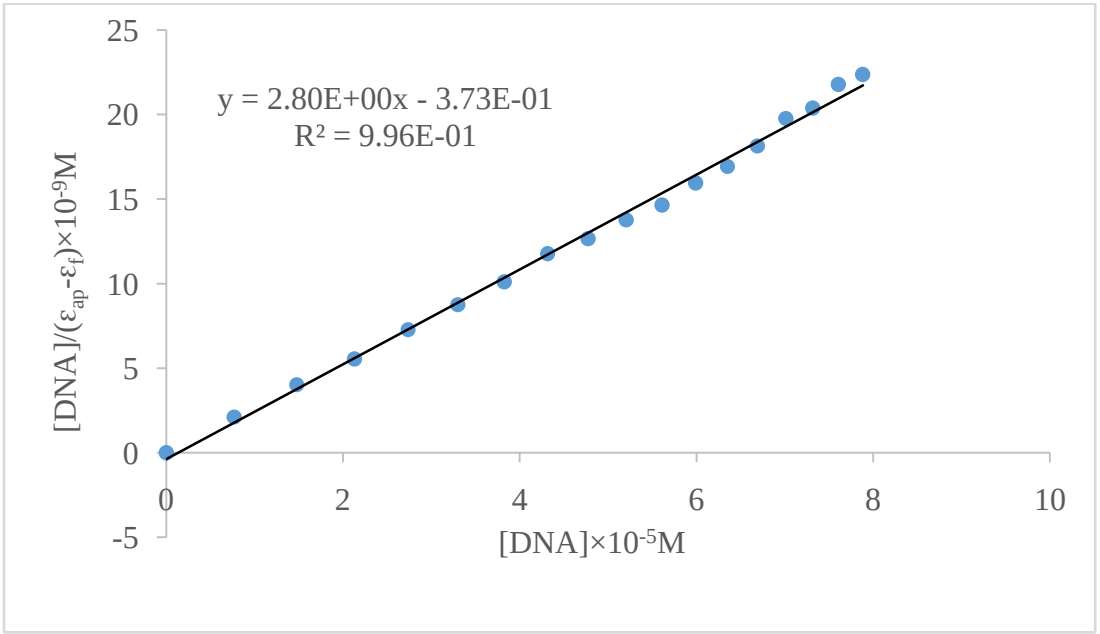

Figure 6: The plot of [ct-DNA]/(ε_{ap}-ε_f) versus [ct-DNA]

Competitive binding studies by fluorescence studies

To investigate the mode of Allura Red AC binding to DNA, a competitive binding experiment was performed. No luminescence was observed for Allura Red AC in the absence or presence of ct-DNA. Ethidium bromide (EB) demonstrates dramatic enhancement of DNA fluorescence efficiency when binds to the ct-DNA. When a second ligand which competed for the DNA binding sites was added, fluorescence quenching was observed [34,35].The interaction of EB with ct-DNA in 5 mM phosphate buffer, pH 7.0 at 25 °C showed by the fluorescence spectra (Fig. 7).

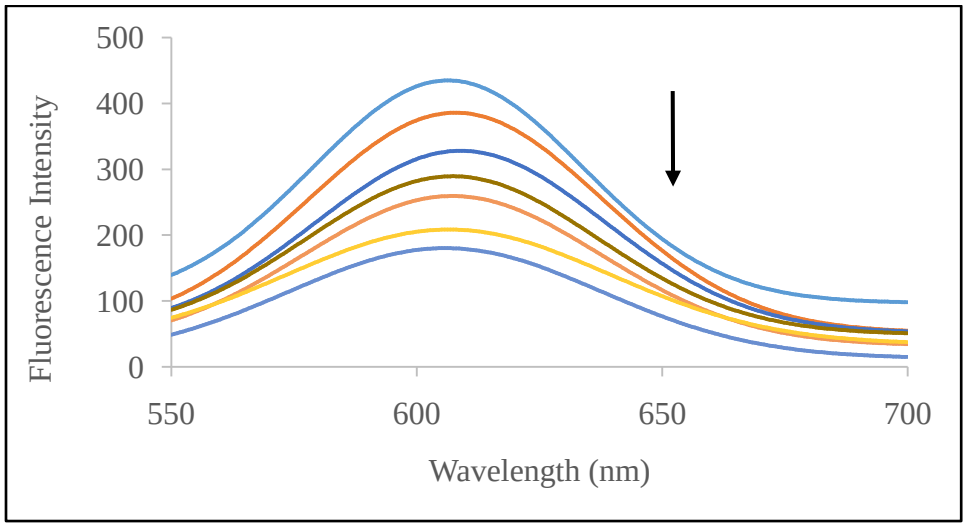

Figure 7: UV-vis spectra of EB (10^{-6} M) in the absence and presence of increasing amounts of ct-DNA

The fluorescent emission of EB (10^{-6}M) bound to ct-DNA (1.3×10^{-5}µM) in the presence of the increasing amounts of the Allura Red AC concentrations shows an decrease in the fluorescence intensity of the EB-ct-DNA. By addition of Allura Red AC to solution of ct-DNA–EB complex, some EB molecules were released into solution after an exchange with the Allura Red AC, and this resulted in fluorescence quenching.

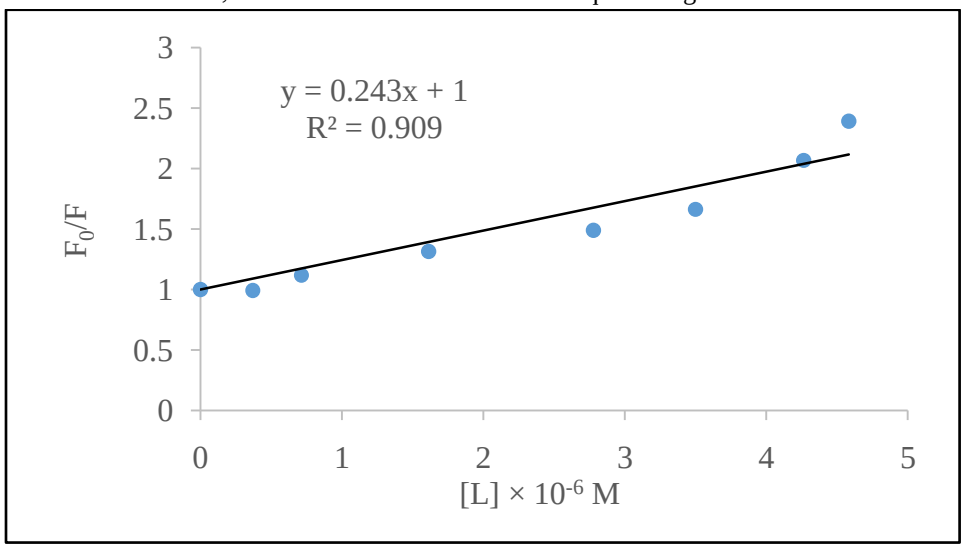

Figure 8: The Stern–Volmer plots of the quenching of fluorescence of Allura Red AC with ct-DNA.

This confirmed the view that Allura Red AC could interact as a groove binder. Fluorescence quenching is described according to the Stern–Vollmer equation (Eq. 2)[35]:

$F_0/F = 1 + K_{SV}[Q]$ (2)

Where F_0 and F represent the emission intensity in the absence and presence of quencher, respectively, K_{SV} is a linear Stern–Vollmer quenching constant and [Q] is the quencher concentration. The Stern–Vollmer quenching plots

from the fluorescence titration data are shown in Fig. 8 and K_{SV} was obtained 0.2438 M^{-1}. When the Stern–Vollmer plot is linear, indicating that only one type of quenching process occurs.

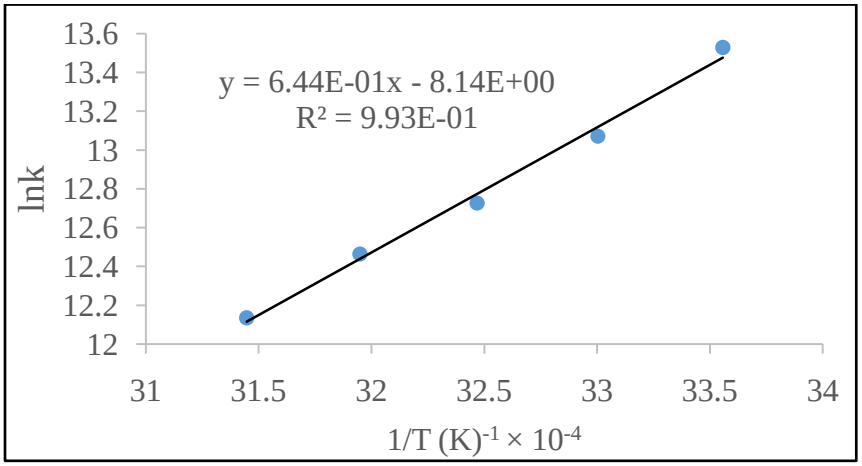

Figure 9: The Stern–Volmer plots of the quenching of fluorescence of Allura Red AC with ct-DNA.

Thermodynamic Studies

The thermodynamic parameters of binding are the main parameters for the confirming the binding force. From the viewpoint of thermodynamics, ΔH > 0 and ΔS > 0 show hydrophobic interaction; ΔH < 0 and ΔS >0 indicate an electrostatic force; ΔH < 0 and ΔS < 0 suggest the van der Waals force and hydrogen bonding [37]. In this study, the formation constant of Allura Red AC–ct-DNA complex formation is calculated at different temperatures, allowing for the determination of thermodynamic parameters by the van't Hoff equation (Eq.3 & Eq.4):

$$\text{Ln } K_b = -\Delta H^o/RT + \Delta S^o/R \quad (3)$$

$$\Delta G^o = \Delta H^o - T\Delta S^o = -RT \text{ Ln } K_b \quad (4)$$

Where K_b is the binding constant at the corresponding temperature and R is the gas constant. The plot of ln K_b versus 1/T allows the determination of ΔHº and ΔSº (Fig.10).

The thermodynamic parameters (ΔH°, ΔS° and ΔGº) for the interaction of the Allura Red ACto ct-DNA are summarized in Table.1.

Table 1: Thermodynamic Parameters of Interaction of Allura Red AC with ct- DNA in 5 mM Phosphate Buffer, pH 7.0 at various temperatures

T(K)	Ln K	ΔG (KJ/mol)	ΔH (KJ/mol)	ΔS (J/mol)
298	13.52872174±0.0339	-33.51838218±5.20	-53.54216±2.64	-67.1938853±8.6
303	13.07107008±0.0163	-32.92788162±5.25		-68.03392205±8.6
308	12.72624077±0.0007	-32.58823475±5.29		-68.03222484±8.6
313	12.46441983±0.0172	-32.43593536±5.33		-67.4320276±8.6
318	12.13510323±0.0332	-32.08341694±5.38		-67.48032409±8.6

It can be seen that the negative sign for ΔGº values revealed the interaction process is spontaneous. We applied this analysis to the binding of Allura Red AC to ct-DNA and found that ΔH < 0 and ΔS < 0. Therefore, van der Waals interactions or hydrogen bonds are the main forces involved in the binding process [38].

Viscosity Study

Hydrodynamic data such as viscosity measurement as an effective test used for understanding of binding mode in the absence of structural data such as X-ray and NMR [39]. A classical intercalation binding requires the space of adjacent base pairs to accommodate the ligand, leading to an increase of DNA viscosity [40]. In contrast, there is little effect on the viscosity of DNA if electrostatic or groove binding occurs in the binding process [41]. The changes in relative viscosity of ct-DNA$(\eta/\eta_0)^{1/3}$ vs. r_i (r_i = [Allura Red AC]/ [ct-DNA]) (where η_0 and η are the specific viscosity of ct-DNA in the absence and in the presence of the Allura Red AC dye, respectively are shown in Fig. 10. It can be seen that the relative viscosity of DNA does not change significantly with increasing of Allura Red

AC concentration. This type of change in viscosity suggested that groove binding should be the interaction mode of Allura Red AC with ct-DNA [42].

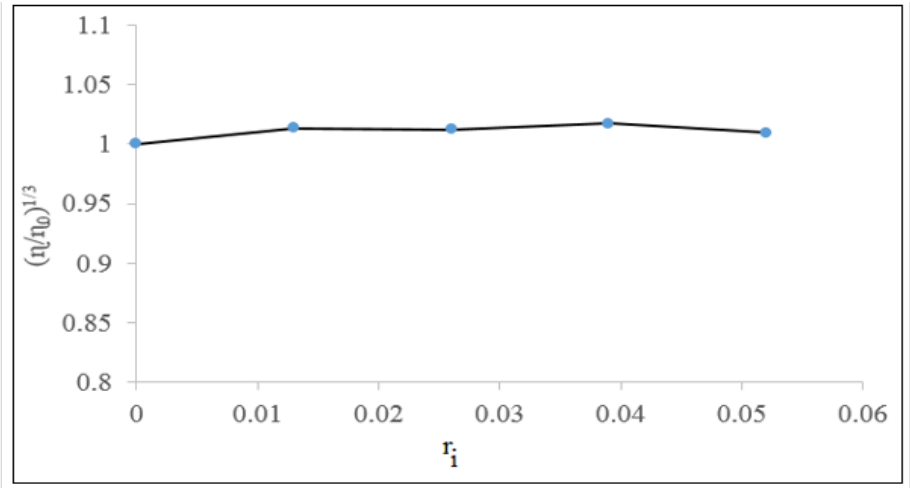

Figure 10: Effect of increasing amounts of Allura Red AC on the viscosity of ct-DNA (1.2×10^{-5} M) in in 5 mM Phosphate Buffer, pH 7.0 at various molar ratios (r_i= [Allura Red Ac]/[ct-DNA], r_i= 0, 0.013, 0.026,0.039 and 0.052)

Thermal denaturation Study

The dissociation of double helix DNA into two single strands results in significant hyperchromism at 260 nm, which depending on the strength and mode of its interaction with the nucleic acid increase denaturation temperatures of DNA. It has been reported that intercalation of small molecules into the double helix DNA is known to increase T_m significantly, while groove binding or electrostatic interaction mode are known to have little effect on T_m [43]. In this study, the thermal denaturation temperature of ct-DNA in the absence and presence of the Allura Red AC are illustrated in Fig.12.

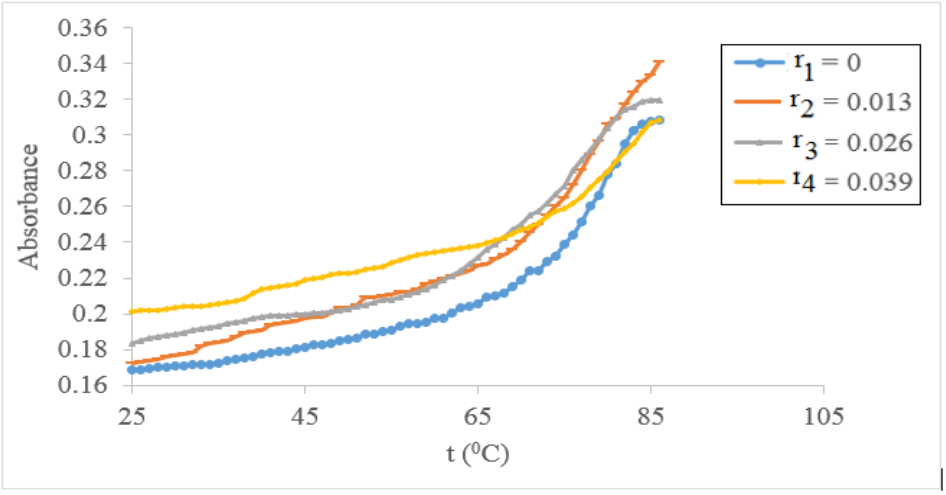

Figure 12: Melting profiles (λ = 260 nm) at various molar ratios (r = [Allura Red Ac]/[ct-DNA]), r_1 = 0.0 (●), r_2 = 0.013 (−), r_3 = 0.026 (▲) and r_4 = 0.039 (♦) in 5 mM Phosphate buffer, pH 7 and in the temperature range of 25°C-86 °C.

The T_m value for the free ct-DNA is 80°C under our experimental conditions. A small change (1 to 5 °C) in the ct-DNA melting temperature on addition of the Allura Red AC was observed (Table.2). The low ΔT_mvalues showed that the Allura Red AC interact with ct-DNAby non-intercalative mode.

Table 2: Melting temperature of free ct-DNA in the absence and in the presence of various stoichiometric ratios (r = [Allura Red AC]/[ct-DNA]).

R=[Allura Red AC]/[ct-DNA]	T_m/K
0	353
0.013	354
0.026	350
0.039	358

Conclusion

The interactions of azo dye,Allura Red AC with ct-DNA was investigated by multi spectroscopic techniques. The results of UV-vis absorption and fluorescence spectroscopy indicated that groove binding mode exists between Allura Red AC and ct-DNA. Moreover, DNA melting studies and viscosity measurement confirmed the groove binding mode of Allura Red AC with ct-DNA. Analysis of the binding between Allura Red AC and ct-DNA will help to better understand the biologically-mediated environmental processes of azo dyes as food colorants.

Acknowledgements

We are grateful to the Research Council of Payame Noor University for their financial supports.

References

1. Kathiravan A, Renganathan R. Photoinduced interactions between colloidal TiO_2 nanoparticles and calf thymus-DNA. *Polyhedron*. 2009, 28: 1374–1378.
2. Zhang G, Ma Y. Spectroscopic studies on the interaction of sodium benzoate, food Preservative with calf thymus DNA. *Food. Chemistry*. 2013, 141:41–47.
3. Nordell P, Lincoln P. Mechanism of DNA Threading Intercalation of Binuclear Ru Complexes: Uni- or Bimolecular Pathways Depending on Ligand Structure and Binding Density. *Journal of the American Chemical Society.* 2005,127:9670-9671.
4. Cheng CC, FuW CH, Hung KC, Chen PJ, Wang WJ, Chen YT. Mechanistic aspects of Co^{II} $(HAPP)(TFA)_2$ in DNA bulge-specific recognition. *Nucleic Acid Research*. 2003, 31: 2227-2233.
5. Mokhir AA, Kraemer R. Conjugates of PNA with Naphthalene Diimide Derivatives Having a Broad Range of DNA Affinities. *Bioconjugate Chemistry*. 2003, 14: 877-883.
6. Tse WC, Boger DL. A Fluorescent Intercalator Displacement Assay for Establishing DNA Binding Selectivity and Affinity. *Accounts of Chemical Research*. 2004, 37: 61-69.
7. Yang P, Ren R, Guo ML, Song AX, Meng XL, Yuan CX, Zhou QH, Chen HL, Xiong ZH, Gao XL. Double-strand hydrolysis of DNA by a Magnesium (II) complex with diethylenetria mine. *Journal of Biological Inorganic Chemistry.*2004, 9: 495-506.
8. Chaviara ATh, Cox PJ, Repana KH, Pantazaki AA, Papazisis KT, Kortsaris AH, Kyriakidis DA, Nikolov GS, Bolos CA. The unexpected formation of biologically active Cu (II) Schiff mono-base complexes with 2-thiophene-carboxaldehyde and dipropylenetriamine: Crystal and molecular structure of Cudpta SCl_2. *Journal of Inorganic Biochemistry.* 2005, 99: 467-476.
9. Pyle AM, Rehmann JP, Meshoyrer R, Kumar CV, Turro NJ, Barton JK. Molecular Mixed-ligand complexes of ruthenium (II): factors governing binding to DNA. *Journal of the American Chemical Society.*1989, 111:3051-3058.
10. Satyanarayana S, Dabrowiak JC, Chaires JB. Neither DELTA nor LAMBDA tris (phenanthroline) Ruthenium (II) binds to DNA by classical intercalation. *Biochemistry*. 1992, 31: 9319-9324.
11. Natansohn A, Rochon P. Photoinduced motions in azo-containing polymers. *Chemical Review*. 2002, 102: 4139–4176.
12. Natansohn A, Rochon P. Photoinduced Motions in Azobenzene-based Polymers, Amsterdam, Academic Press, 2002.
13. Rau H. Photochemistry and Photophysics, Boca Raton, CRC Press, 1990.

14. Pinheiro H M, Touraud E, Thomas O. Aromatic amines from azo dye reduction: status review with emphasis on direct UV spectrophotometric detection in textile industry wastewaters. *Dyes and Pigment*. 2004, 61:121–139.
15. Gordon P F, Gregory P. Polyene and Polymethine, Berlin, Springer, 1987.
16. King-Thom C. Mutagenicity and Carcinogenicity of Aromatic Amines Metabolically Produced from Azo Dyes. *Journal of Environmental Science and Health, Part C.*2000, 18: 51-74.
17. Pahdi B S. Pollution due to synthetic dyes toxicity & carcinogenicity studies and remediation. *International Journal of Environmental Science*. 2012, 3: 940-955.
18. Chowdhury G. Human health perspectives on environmental exposure to benzidine: A review. *Chemosphere*. 1996, 32: 267-291.
19. Liamas N S, Garrido M, Nezio M S D, Band B S F. Second order advantage in the determination of amaranth, sunset yellow FCF and tartrazine by UV–vis and multivariate curve resolution-alternating least squares. *Analytica Chimica Acta.* 2009, 655: 38-42.
20. Zhang G, Ma Y. Mechanistic and conformational studies on the interaction of food dye Amaranth with human serum albumin by multispectroscopic methods. *Food Chemistry*. 2013, 136: 442-449.
21. Mpountouk P, Pantazaki A, Kostareli E, Christodoulou P, Kareli D, Poliliou S, Mourelatos C, Lambropoulou V, Lialiaris T. Cytogenetic evaluation and DNA interaction studies of the food colorants Amaranth, erythrosine and tatrazine. *Food and Chemical Toxicology*. 2010, 48:2934-2944.
22. Shahabadi N, Maghsudi M, Rouhani Sh. Study on the interaction of food colourant quinolone yellow with bovine serum albumin by spectroscopic techniques. *Food Chemistry*. 2012, 135: 1836-1841.
23. Amjad H El-Sheikh, Yahya S Al-Degs. Spectrophotometric determination of food dyes in soft drinks by second order multivariate calibration of the absorbance spectra-pH data matrices. *Dyes and Pigments*. 2013, 97: 330-339.
24. Ribo JM, Crusats J, Farrera JA, Valero ML. Aggregation in water solutions of tetrasodium diprotonated *meso*-tetrakis (4-sulfonatophenyl) porphyrin. *Journal of the Chemical Society Chemical Communications*. 1994:681-682.
25. Bordbar AK, Eslami A, Tangestaninejad Sh. Spectral Investigation on Solution Properties of 5, 10, 15, 20-Tetrakis (N-Benzyl-4-Pyridyl) Porphyrin due to Its Interaction with Human Serum Albumin. *Journal of Porphyrins and Phthalocyanines*. 2002, 6: 225-232.
26. Barber DC, Freitage-Beeston RA, Whitten DG. Atropisomer-specific formation of pre micellar porphyrin J-aggregates in aqueous surfactant solutions. *Journal of Physical Chemistry A.*1991, 95: 4074-4086.
27. Liu Y, Zhang K, Wu Y, Zhao J, Liu J. Antioxidation and DNA-Binding Properties of Binuclear Lanthanide(III) Complexes with a Schiff Base Ligand Derived from 8-Hydroxyquinoline-7-carboxaldehyde and Benzoylhydrazine. *Chemistry & Biodiversity*. 2012, 9: 1533–1544.
28. Li QS, Yang P, Wang HF, Guo ML. Diorganotin(IV) antitumor agent. $(C_2H_5)_2$ $SnCl_2$ (phen) =nucleotides aqueous and solid-state coordination chemistry and its DNA binding studies. *Journal of Inorganic Biochemistry.*1996, 64: 181–195.
29. Shahabadi N, Kashanian S, Mahdavi M, Sourinejad N. DNA Interaction and DNA Cleavage Studies of a New Platinum (II) Complex Containing Aliphatic and Aromatic Dinitrogen Ligands. *Bioinorganic Chemistry and Applications*. 2011: 525794.
30. Shoair AF, El-Shobaky AR, Azab EA. Synthesis, characterization, DNA binding and catalytic applications of Ru(III) complexes. *Spectrochimica Acta Part A.* 2015, 151: 322–334.
31. Costes JP, Dahan F, Laurent J P, Drillon M. An alternating Copper (II) chain with bridging oxamidato and nitrito ligands: crystal structure and magnetic properties of $[Cu\ (NO_2)_2CuL]_{(n)}$ (L = N,N'-bis(2-methyl-2-aminopropyl) oxamide. *Inorganica Chimica Acta*. 1999, 294:8–13.
32. Arjmand F, Sayeed F. Synthesis, characterization and DNA-binding studies of mono and heterobimetallic complexes Cu [single bond] Sn_2/Zn{single bond}Sn_2 and their DNA cleavage activity. *Journal of Molecular Structure.* 2010, 965: 14-22.

33. Shahabadi N, Kashanian S, Darabi F. DNA binding and DNA cleavage studies of a water soluble Cobalt (II) complex containing dinitrogen Schiff base ligand: The effect of metal on the mode of binding. *European Journal of Medicinal Chemistry.* 2010, 45: 4239-4245.
34. Baguley BC, Lebret M. Quenching of DNA-ethidium fluorescence by amsacrine and other antitumor agents: a possible electron-transfer effect. *Biochemistry*. 1984, 23: 937-943.
35. Lakwociz JR, Webber G. Quenching of fluorescence by oxygen. A probe for structural fluctuations in macromolecules. *Biochemistry*. 1973, 12: 4161-4170.
36. Guan Y, Zhou W, Yao X. Determination of nucleic acids based on the fluorescence quenching of Hoechst 33258 at pH 4.5. *Analytica Chimica Acta.*2006, 570: 21–28.
37. Wu SS, Yuan WB, Wang HY, Zhang Q , Liu M, Yu KB J. Synthesis, crystal structure and interaction with DNA and HSA of (*N,N′*-dibenzylethane-1,2-diamine) transition metal complexes. *Inorganic Biochemistry*. 2008, 102: 2026-2034.
38. Hemmateenejad B, Shamsipour M, Samari F, Khayamian T, Ebrahimi M, Rezaei Z. Combined fluorescence spectroscopy and molecular modeling studies on the interaction between harmalol and human serum albumin. *Journal of Pharmaceutical and Biomedical Analysis*. 2012, 67: 201-208.
39. Satyanarayana S, Dabrowiak JC, Chaires JB. Neither delta- nor lambda-tris(phenanthroline)ruthenium(II) binds to DNA by classical intercalation. *Biochemistry*. 1992, 31: 9319-9324.
40. Lerman L S. Structural considerations in the interaction of DNA and acridines. *Journal of Molecular Biology.*1961, 3: 18–30.
41. Zhang G, Fu P, Pan J. Multispectroscopic studies of paeoniflorin binding to calf thymus DNA *in vitro*. *Journal of Luminescence*. 2013, 134: 303–307.
42. Mahadevan S, Palaniandavar M. Spectroscopic and Voltammetric Studies on Copper Complexes of 2,9-Dimethyl-1,10-phenanthrolines Bound to Calf Thymus DNA. *Inorganic Chemistry.*1998, 37: 693-700.
43. Zeyneb D, Ralph P, Jan ARS, Sukunath N, Clemens R. 5‘-Tethered Stilbene Derivatives as Fidelity- and Affinity-Enhancing Modulators of DNA Duplex Stability. *Journal of the American Chemical Society*.2004, 126: 4762-4763.